NASA TECHNICAL NOTE

NASA TN D-2877

NASA TN D-2877

SOME NONASYMPTOTIC EFFECTS ON THE SONIC BOOM OF LARGE AIRPLANES

by F. Edward McLean

Langley Research Center

Langley Station, Hampton, Va.

NATIONAL AERONAUTICS AND SPACE ADMINISTRATION • WASHINGTON, D. C. • JUNE 1965

NASA TN D-2877

SOME NONASYMPTOTIC EFFECTS ON THE SONIC BOOM OF LARGE AIRPLANES

By F. Edward McLean

Langley Research Center
Langley Station, Hampton, Va.

NATIONAL AERONAUTICS AND SPACE ADMINISTRATION

For sale by the Clearinghouse for Federal Scientific and Technical Information
Springfield, Virginia 22151 – Price $1.00

SOME NONASYMPTOTIC EFFECTS ON THE SONIC BOOM OF LARGE AIRPLANES

By F. Edward McLean
Langley Research Center

26650

SUMMARY

The study of a number of equivalent bodies representing a large airplane at critical transonic flight conditions indicates the possible inapplicability of the asymptotic far-field theory used in current sonic-boom analyses. At these normal operating conditions the pressure field from a large airplane, such as the supersonic transport, tends to exhibit important nonasymptotic near-field characteristics which must be calculated with the use of general theory. Since the shape and magnitude of the near-field pressure signature is dependent on airplane equivalent body shape, suppression of the sonic boom through a design approach to a more idealized near-field shape is suggested. The results of the study indicate that if certain effective area distributions can be achieved by real airplanes, sonic-boom overpressures much lower than those predicted by current asymptotic methods would be possible.

Author

INTRODUCTION

Sonic boom has become a major problem in the current national program for the development of a commercial supersonic transport. Extensive supersonic overflight of populated areas is envisioned for the transport airplanes; consequently, the associated property damage and annoyance to the population caused by the sonic boom could lead to severe restrictions in airplane design and operation. The effect of these restrictions on the flight characteristics of the airplane, particularly at critical transonic acceleration conditions, might well be the pivotal issue which decides the economic feasibility of the supersonic transport.

The serious nature of the sonic-boom implications in supersonic airplane development has led to considerable research effort to develop analytic methods which accurately describe the relationship between the airplane and its sonic-boom characteristics. In the sonic-boom analysis methods which have evolved from this research, some results of which are summarized in reference 1, the airplane at various lifting conditions has been conveniently represented by equivalent bodies of revolution. The sonic-boom characteristics of these equivalent bodies of revolution have then been determined by use of the asymptotic far-field shock relationships derived by Whitham (ref. 2).

The asymptotic far-field relationship, which is a special solution of more general shock equations derived by Whitham, is a theoretical representation of the pressure disturbances generated by a body of revolution at some location far from the body. Sonic-boom data obtained during the overflights of current supersonic airplanes at normal operating altitudes have correlated reasonably well with these theoretically derived far-field solutions (ref. 1). However, in sonic-boom wind-tunnel experiments it has been difficult to simulate far-field conditions. Even with extremely small models, the N-wave pressure signature which characterizes the far field is generally not fully developed in the distances permitted from the model to the floor of the wind tunnel (ref. 1). In an attempt to overcome this difficulty, consideration was given to the applicability of the general shock relationships of reference 2 in the obvious near-field confines of the wind tunnel. The premise was that if general theory could predict the pressures near an airplane model or its representative equivalent body then these pressures could be extrapolated to the proper far-field condition with confidence. If the feasibility of this extrapolation could be shown, it would be possible to use larger wind-tunnel models with a better representation of the design features of the airplane.

During the early phases of this investigation, an interesting and perhaps more important possibility was indicated by the analysis. This possibility was that, at some critical flight conditions, the pressure field of a large airplane, such as the supersonic transport, would reach a far-field variation only at distances well beyond normal operational altitudes. Under these nonasymptotic conditions the general or near-field solution of the theory indicates lower levels of sonic-boom overpressures than are indicated by the currently accepted far-field solution. Furthermore, since the shape of the pressure signature under nonasymptotic conditions is still influenced by the shape of the airplane equivalent body, the possibility of further sonic-boom suppression through airplane design modifications was suggested. The purpose of the present investigation is to explore some of these nonasymptotic solutions of the sonic-boom theory for large airplanes.

The general theory of reference 2 is applied herein to determine the bow-shock pressure-rise characteristics of several analytic bodies of revolution. Particular emphasis is given to the effect of body shape on the distance from the body at which far-field conditions are effectively attained and on the manner in which the bow-shock pressure rise approaches the asymptotic variation. Test models of several equivalent bodies were designed to represent the combined lift and base-area requirements of a typical 450 000-pound supersonic transport at critical transonic flight conditions (Mach number 1.414). Pressure signatures measured at a Mach number of 1.414 in the near field of the test models are compared with pressure signatures calculated by the general theory of reference 2. The degree to which these theoretical and experimental nonasymptotic near-field pressures approximate the asymptotic values is indicated. Finally the nonasymptotic sonic-boom ground overpressures which would be anticipated from several representative transport equivalent bodies are compared with corresponding asymptotic overpressures and with the asymptotic lower bound of sonic-boom overpressures discussed in references 1 and 3.

SYMBOLS

A cross-sectional area of airplane or model

$A(t)$ nondimensionalized cross-sectional area, A/l^2

A_b cross-sectional area at base of airplane or model

A_e nondimensionalized effective cross-sectional area due to combination of volume and lift effects, $A(t) + B(t)$

$A_{e,b}$ nondimensionalized effective cross-sectional area at base of airplane or model due to combination of base area and lift effects, $\frac{\beta}{2} C_L \frac{S}{l^2} + \frac{A_b}{l^2}$

B equivalent cross-sectional area due to lift, $\frac{\beta}{2q} \int_0^x F_L \, d\xi$

$B(t)$ nondimensionalized equivalent cross-sectional area due to lift, B/l^2

C_L lift coefficient

F_L lifting force per unit length along longitudinal axis of airplane or model

$F(\tau)$ effective area distribution function, $\frac{1}{2\pi} \int_0^\tau \frac{A_e'' \, d\xi}{\sqrt{\tau - \xi}}$

h airplane flight altitude or perpendicular distance from model to measuring probe

$I(\tau)$ effective area distribution integral, $\int_0^\tau F(\eta) d\eta$

K_r reflection factor

$k = \frac{(\gamma + 1)M^4}{\sqrt{2}\beta^{3/2}}$

l airplane or model reference length

M Mach number

p reference pressure for a uniform atmosphere (free-stream static pressure for wind-tunnel tests)

p_a atmospheric pressure at airplane altitude

p_g atmospheric pressure at ground level

Δp incremental pressure due to flow field of airplane or model

q dynamic pressure

S wing planform area

t nondimensionalized distance, x/l

W airplane weight

x distance measured along longitudinal axis from airplane nose or model nose

$\bar{x}$ longitudinal distance from airplane nose or model nose to point on corrected characteristic

ΔX distance from point in undisturbed flow ahead of shock to point on pressure signature

$\beta = \sqrt{M^2 - 1}$

γ ratio of specific heats (1.4 for air)

η dummy variable of integration corresponding to τ

ξ dummy variable of integration corresponding to t

τ nondimensionalized linear theory characteristic variable, $\frac{x - \beta h}{l}$

τ_o value of τ giving largest positive value of $I(\tau)$

A prime is used to indicate a first derivative and a double prime is used to indicate a second derivative with respect to indicated argument of the function.

THEORETICAL CONSIDERATIONS

The theoretical studies of reference 2 have provided a means for estimating the pressures at any point in the supersonic flow field about an axisymmetric body of revolution. In the adaptations of this method for consideration of the complex flow patterns about an asymmetric airplane configuration at lifting conditions, the volume and lift distributions have been combined to form a representative equivalent body of revolution (refs. 1 and 4). The effective area distribution of the assumed equivalent body of revolution is given by

$$A_e = A(t) + B(t) \tag{1}$$

The term $A(t)$ in equation (1) represents a distribution along the longitudinal axis of a nondimensionalized airplane cross-sectional area and is generally obtained from supersonic area-rule concepts. The term $B(t)$ represents a distribution of nondimensionalized equivalent area due to lift evaluated through an integration of the lifting force per unit length along the airplane longitudinal axis. The effective nondimensionalized base area $A_{e,b}$ can be expressed as

$$A_{e,b} = \frac{\beta C_L S}{2l^2} + \frac{A_b}{l^2} = \frac{\beta W}{2ql^2} + \frac{A_b}{l^2} \tag{2}$$

The first term of $A_{e,b}$ depends on the weight and operating condition of the airplane; since the physical area of an efficient airplane generally approaches zero at the base, the term A_b depends primarily on the jet exit area of the airplane engines.

A function $F(\tau)$, related to the body area distribution, is essential in the method of reference 2. If the area distribution due to volume used in the derivations of reference 2 can be replaced by an effective area due to volume and lift, the function $F(\tau)$ can be expressed as

$$\left.\begin{aligned} F(\tau) &= \frac{1}{2\pi} \int_0^\tau \frac{A_e'' \, d\xi}{\sqrt{\tau - \xi}} \\ F(\tau) &= \frac{1}{2\pi} \int_0^\tau \frac{dA_e'}{\sqrt{\tau - \xi}} \end{aligned}\right\} \tag{3}$$

where the latter expression is a Stieltjes integral which can be used for discontinuous slopes if the Lighthill correction (ref. 2) is applied near the point of discontinuity. However, a sharp discontinuity in the forward area development is undesirable from drag considerations, and the boundary layer tends to fair over minor discontinuities. For efficient supersonic airplanes the major effect of discontinuities is expected to be restricted to the wake-induced pressure field.

Once the function $F(\tau)$ is determined from equations (3), a description of the entire flow field about a body of revolution is possible with the method of reference 2. For convenience two zones of influence may be considered: in the near field of the body of revolution, body shape (or the shape of $F(\tau)$) has an influence on the shape of the pressure signature, and, in the asymptotic far field, body shape no longer has an influence on the shape of the pressure signature or on the rate of decrease of the shock strength with distance. Although reference 2 contains a complete description of the theory, the

relationships pertinent to the present analysis are included herein in the notation of the present paper.

General Theory Expressions for Pressure Signature

For any effective area distribution A_e which generates an $F(\tau)$ function with one region of compression $F'(\tau) > 0$ in the positive range of $F(\tau)$ and one region of compression in the negative range of $F(\tau)$, the flow field will be characterized by two shocks. Such an $F(\tau)$ function is shown in figure 1(a). If it is desired to locate the shocks at some radial distance h/l from the body which generated the illustrated $F(\tau)$ function, τ_1, τ_2, τ_3, and τ_4 must be determined such that

$$k\left(\frac{h}{l}\right)^{1/2} = \frac{\tau_2 - \tau_1}{F(\tau_2)} = \frac{\tau_4 - \tau_3}{F(\tau_4) - F(\tau_3)} \tag{4}$$

Also, the following conditions must be met at the bow shock:

$$I(\tau_2) = \frac{1}{2}(\tau_2 - \tau_1)\left[F(\tau_2)\right] \tag{5}$$

and at the tail shock:

$$I(\tau_4) - I(\tau_3) = \frac{1}{2}(\tau_4 - \tau_3)\left[F(\tau_4) + F(\tau_3)\right] \tag{6}$$

The solutions of equations (4) and (5) for the bow shock and (4) and (6) for the tail shock are equivalent to passing lines of slope $\frac{1}{k(h/l)^{1/2}}$ through the curve for $F(\tau)$ as illustrated in figure 1(a) such that Area I = Area II and Area III = Area IV.

With τ_1, τ_2, τ_3, and τ_4 defined, the pressure signature at the desired h/l is given by

$$\left.\begin{aligned} \left(\frac{\Delta p}{p}\right) &= \frac{K_r \gamma M^2 F(\tau)}{\sqrt{2\beta}(h/l)^{1/2}} \\ \frac{\bar{x} - \beta h}{l} &= \tau - kF(\tau)\left(\frac{h}{l}\right)^{1/2} \end{aligned}\right\} \quad \begin{pmatrix} \tau_2 \leqq \tau \leqq \tau_3 \\ \tau_4 \leqq \tau \leqq \infty \end{pmatrix} \tag{7}$$

where τ_2 defines the bow shock and τ_3 and τ_4 define the tail shock. The term K_r in equation (7) is a reflection factor used in current sonic-boom

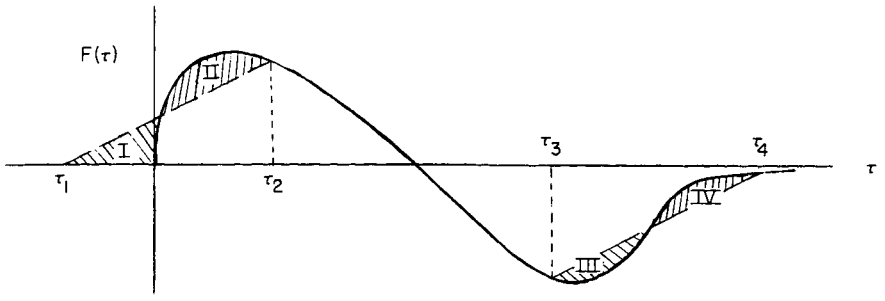

(a) Effective area distribution function $F(\tau)$.

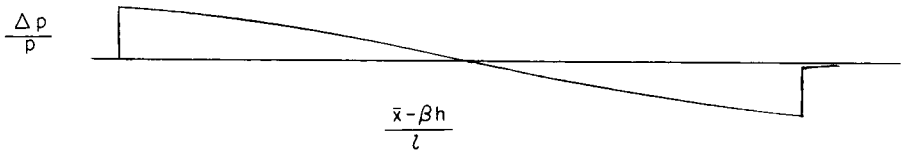

(b) Pressure signature.

Figure 1.- Representative effective area distribution function and general theory pressure signature.

analyses which has a value of unity until the pressure wave comes in contact with a reflective surface. A representative pressure signature obtained from a solution of the general theory equations is illustrated in figure 1(b).

If only the bow shock characteristics are of interest, the solution can be written such that the strength, or pressure jump at the bow shock, is given by

$$\left(\frac{\Delta p}{p}\right)_{\text{bow shock}} = \frac{1.075\beta^{1/4}K_r\left[I(\tau)\right]^{1/2}}{\left(\frac{h}{\ell}\right)^{3/4}_{\text{bow shock}}} \tag{8}$$

where

$$\left(\frac{h}{\ell}\right)_{\text{bow shock}} = \frac{4\left[I(\tau)\right]^2}{k^2\left[F(\tau)\right]^4} \tag{9}$$

and

$$I(\tau) = \int_0^{\tau} F(\eta)d\eta \tag{10}$$

The bow shock is located at a longitudinal position given by

$$\frac{\bar{x} - \beta h}{l} = \tau - kF(\tau)\left(\frac{h}{l}\right)^{1/2}_{\text{bow shock}} \tag{11}$$

As τ is increased in the positive region of $F(\tau)$, the bow-shock characteristics are described at greater and greater distances from the generating body. (See eqs. (8) to (10).) If one follows this general solution from the vicinity of the generating body outwards, the influence of the shape of $F(\tau)$ and hence A_e on $\left(\frac{\Delta p}{p}\right)_{\text{bow shock}}$ and $\left(\frac{h}{l}\right)_{\text{bow shock}}$ diminishes. Finally a radial distance given by

$$\left(\frac{h}{l}\right)_{\text{bow shock}} = \frac{4\left[I(\tau_o)\right]^2}{k^2\left[F(\tau_o)\right]^4} \tag{12}$$

is reached at which the body shape no longer has an influence on the shape of the pressure signature. At this so-called far-field location a typical N-wave pressure develops and the general solution is replaced by an approximate asymptotic expression. If $F(\tau) \to 0$ as $\tau \to \tau_o$, the bow shock would reach far-field conditions only at an infinite radial distance from the body. (See eq. (12).) If $F(\tau)$ is finite but discontinuous at $\tau = \tau_o$ the radial distance from the body required for asymptotic pressure variation can be determined from equation (12) with the use of the largest positive value of $F(\tau_o)$.

Asymptotic Expression for Bow-Shock Pressure Rise and Pressure Signature

The asymptotic expression for the bow-shock pressure rise in the far field may be determined by the use of equation (8) as

$$\left(\frac{\Delta p}{p}\right)_{\text{bow shock}} = \frac{1.075\beta^{1/4}K_r\left[I(\tau_o)\right]^{1/2}}{\left(\frac{h}{l}\right)^{3/4}} \tag{13}$$

and the asymptotic bow shock is located at a longitudinal position given by

$$\frac{\bar{x} - \beta h}{l} = \tau_o - \left\{2k\left[I(\tau_o)\right]\right\}^{1/2}\left(\frac{h}{l}\right)^{1/4} \tag{14}$$

In equation (13), $\left(\frac{\Delta p}{p}\right)_{\text{bow shock}}$ is dependent on the body shape or the

longitudinal variation of A_e only as a constant $I(\tau_o)$ which is related to A_e. Also, the shock strength varies as $\left(\frac{h}{l}\right)^{-3/4}$ irrespective of the shape of A_e.

In the far field,

$$\left(\frac{\Delta p}{p}\right)_{\text{tail shock}} = -\left(\frac{\Delta p}{p}\right)_{\text{bow shock}}$$

and the tail shock is located at a longitudinal position given by

$$\frac{\bar{x} - \beta h}{l} = \tau_o + \left\{2k\left[I(\tau_o)\right]\right\}^{1/2}\left(\frac{h}{l}\right)^{1/4} \tag{15}$$

The pressure varies linearly between the values at the bow and tail shocks.

RESULTS AND DISCUSSION

Equations (8), (9), and (12), which are based on the general theory of reference 2, indicate that body shape, through its influence on $F(\tau)$, has an effect on the distance from the body at which asymptotic pressure conditions are essentially attained. For certain types of area distribution the theoretical distance from the body to the far field can be uniquely determined from equation (12). The general theory equations indicate a further influence of body shape on the manner in which the bow-shock pressure-rise characteristics approach an asymptotic far-field variation. A number of analytic equivalent bodies of revolution are used herein to consider the possible importance of these effects which have not been considered in sonic-boom analyses of supersonic airplanes at normal operating conditions.

Effect of A_e on Approach to Asymptotic Far-Field Conditions for Pointed Bodies

With the use of general theory equations (8) and (9), the bow-shock pressure-rise parameter $\dfrac{\left(\frac{\Delta p}{p}\right)_{\text{bow shock}}\left(\frac{h}{l}\right)^{3/4}}{\beta^{1/4}K_r}$ for the series of pointed bodies $\left(\text{viz, } A_e'(0) = 0\right)$ represented in figure 2 have been determined at a Mach number of 1.414. The calculated general theory pressure-rise parameter divided by $\sqrt{A_{e,b}}$ for these bodies is shown in figure 3 plotted against a distance

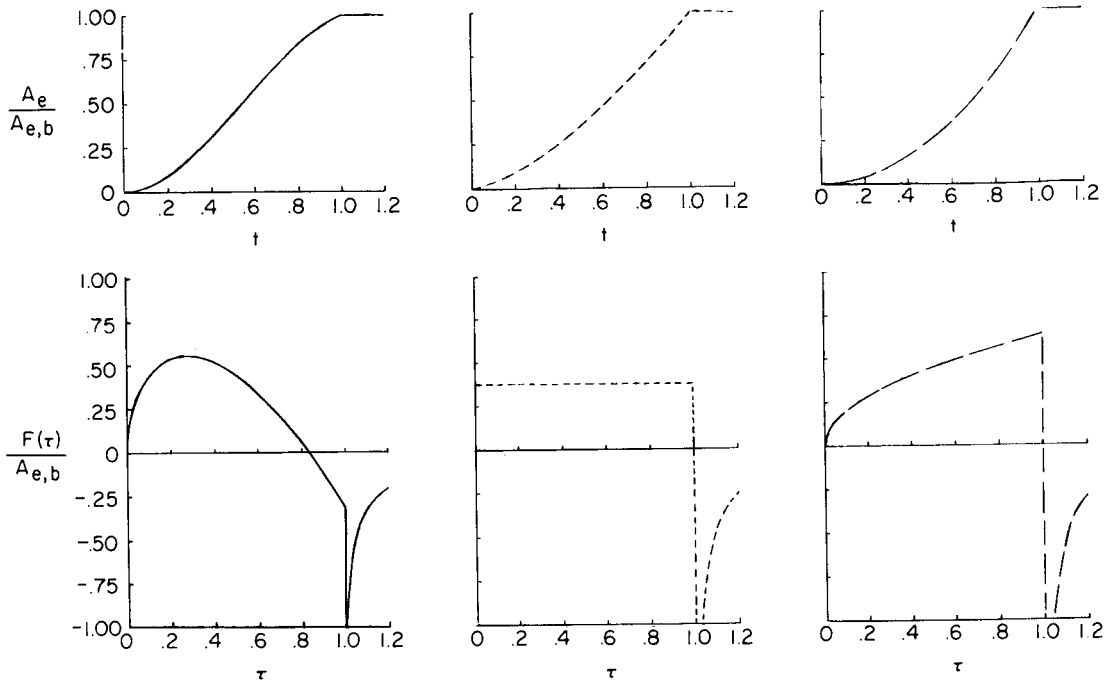

(a) $A_e = A_{e,b}(2.5t^2 - 1.5t^3)$. (b) $A_e = A_{e,b}(t)^{3/2}$. (c) $A_e = A_{e,b}(t)^2$.

Figure 2.- Effective area distribution and effective area distribution function for pointed bodies.

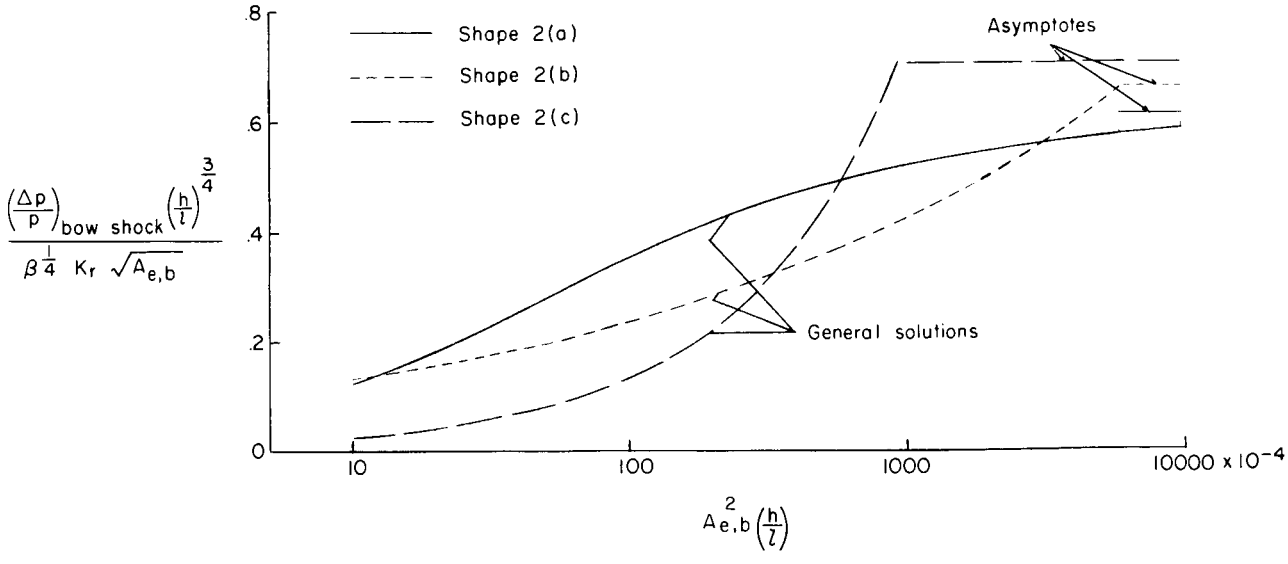

Figure 3.- Variation of bow-shock pressure-rise parameter with distance parameter for pointed bodies. M = 1.414.

parameter $A_{e,b}^2\left(\frac{h}{l}\right)$. Also shown are the asymptotic far-field pressure-rise parameters for each of the three shapes. The asymptotic values are invariant with distance parameter.

From figure 3, the shape of the effective area distribution A_e has a marked influence on the manner in which the bow-shock pressure-rise parameters approach their respective asymptotes. Since the effective area shape shown in figure 2(a) has an $F(\tau)$ distribution which approaches zero as τ approaches τ_o, the far-field solution is a true asymptote. For the effective area shapes shown in figures 2(b) and 2(c), which have discontinuous non-zero values of $F(\tau)$ at τ_o, the theoretical distance to the far field can be determined from equation (12) for a specified $A_{e,b}$ and body length. The bow-shock pressure rise for the shape shown in figure 2(c) does not represent the maximum overpressure which would be present in the signature because $F(\tau)$ for the shape shown in figure 2(c) increases as τ increases. For convenience, the shapes shown in figures 2 and 4 are identified hereinafter by figure number.

The fact that h/l and $A_{e,b}$ are factors of the abscissa in figure 3 indicates the possible inapplicability of the currently used asymptotic solutions in the sonic-boom analysis of a long slender airplane such as the supersonic transport. The curves of figure 3 further suggest that sonic-boom advantages may accrue if the effective area distribution of an airplane is such that nonasymptotic near-field pressure-rise characteristics are provided at normal operating conditions.

Effect of A_e on Approach to Asymptotic Far-Field Conditions for Blunt Bodies

General theory calculations similar to those for the pointed bodies of figure 2 have been made for the series of blunt bodies $\left(\text{viz, } A_e'(0) > 0\right)$ represented in figure 4. Although these blunt effective area shapes would probably be impractical from drag considerations, they are of interest since the lower bound asymptote of sonic-boom overpressures is obtained from one of these shapes (shape 4(a)). This lower bound shape, which was derived in reference 3, is not amenable to exact solution because of the extreme nose bluntness. However, a limiting solution can be obtained which indicates that the positive $F(\tau)$ pulse is located at the nose with zero values over the remainder of the body length (ref. 3). An integration of the limiting solution yields the lower bound asymptotic bow-shock pressure-rise parameter of $0.54\sqrt{A_{e,b}}$. Since $F(\tau)$ is infinite at $\tau = \tau_o$, equation (12) would indicate that the bow-shock pressure-rise characteristics for this lower bound shape would essentially reach asymptotic conditions at the body.

The variation with distance of the bow-shock pressure-rise parameter divided by $\sqrt{A_{e,b}}$ of the blunt bodies of figure 4 is shown in figure 5. As

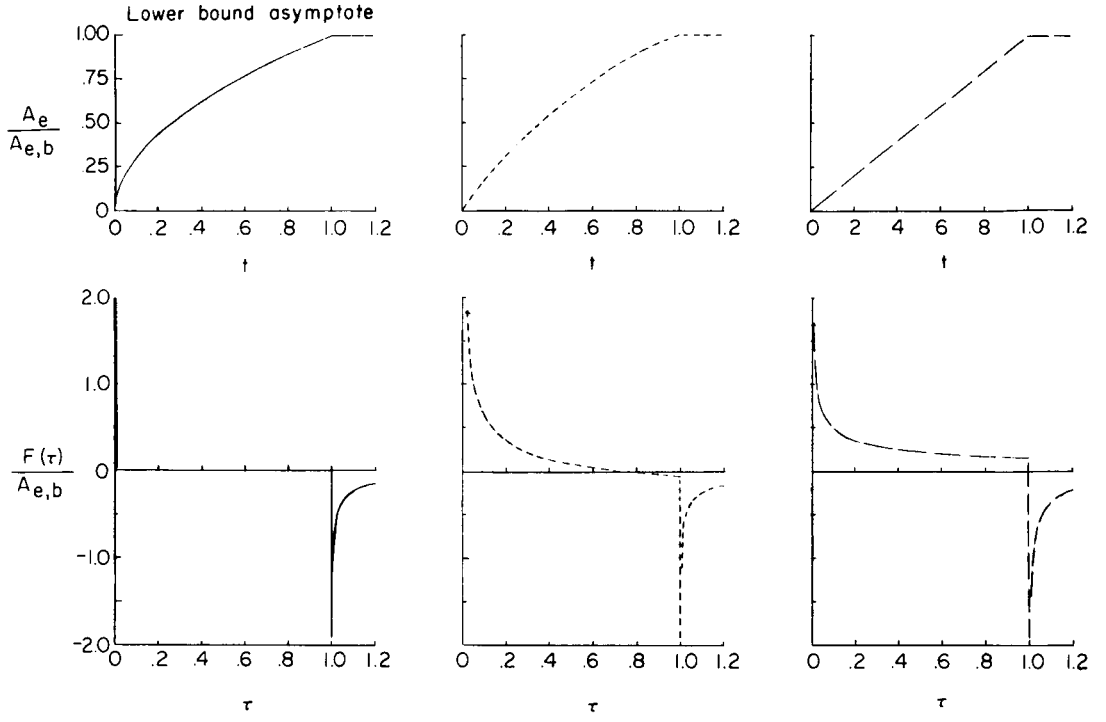

Figure 4.- Effective area distributions and effective area distribution function for blunt bodies.

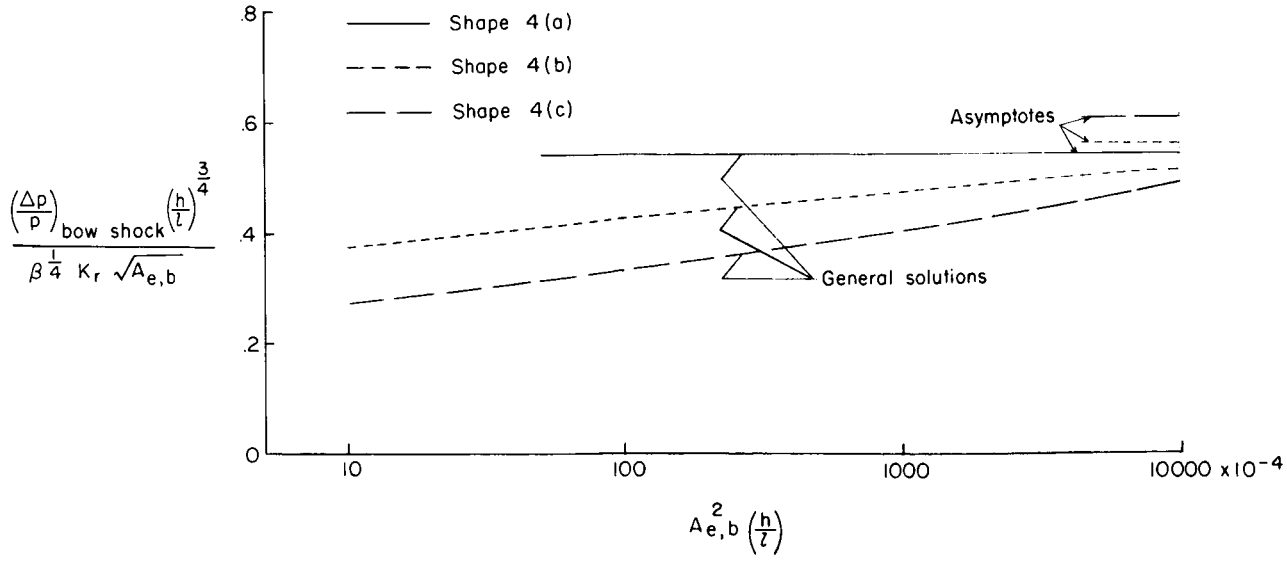

Figure 5.- Variation of bow-shock pressure-rise parameter with distance parameter $A_{e,b}^2\left(\frac{h}{l}\right)$ for blunt bodies. M = 1.414.

might be expected, shapes 4(b) and 4(c) have higher asymptotic pressure-rise levels than does the lower bound shape 4(a). However, at distances before the far-field condition is reached, shapes 4(b) and 4(c) have substantially lower bow-shock pressures than would be predicted from lower-bound considerations. As for the pointed bodies, figure 5 indicates that the shape of A_e has a marked influence on the manner in which the bow-shock pressure-rise approaches an asymptotic far-field variation.

Dimensional Consideration of Possible Nonasymptotic Effects

The results of figures 3 and 5 suggest that for critical transonic acceleration conditions, a long slender airplane such as the supersonic transport might generate a nonasymptotic near-field pressure signature at the ground. If this is so then the far-field expression (eq. (13)) normally used in sonic-boom estimates could overpredict the sonic-boom ground overpressures for this critical condition. In order to pursue this possibility, representative dimensions must be applied to the curves of figures 3 and 5. A typical large supersonic transport configuration with $l = 230$ feet and $W = 450\,000$ pounds in transonic flight ($M = 1.414$) at an altitude of 44,000 feet would have an effective nondimensionalized base area $A_{e,b}$ of 0.01 corresponding to a body with a ratio of length to base diameter of 8.86.

With these representative values of $A_{e,b}$ and l, some of the curves of figures 3 and 5 have been redrawn for the assumed operating condition. The bow-shock pressure-rise parameter $\dfrac{\left(\frac{\Delta p}{p}\right)_{\text{bow shock}}\left(\frac{h}{l}\right)^{3/4}}{\beta^{1/4}K_r}$, corresponding to the assumed size and flight conditions, is shown as a function of h in figure 6.

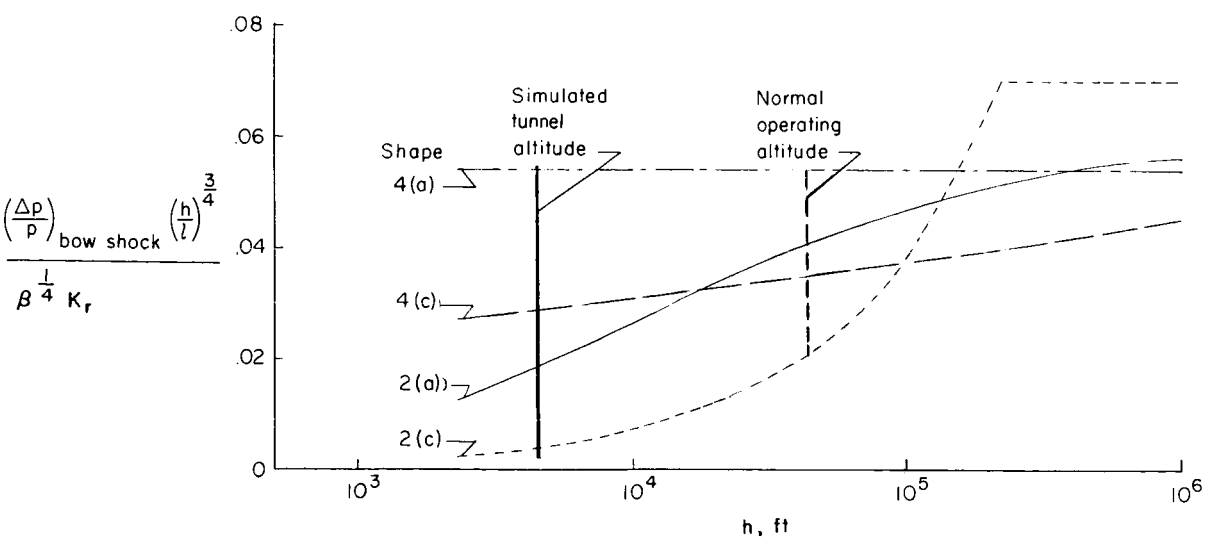

Figure 6.- Variation of bow-shock pressure-rise parameter with h for typical supersonic transport dimensions and operating condition. $M = 1.414$; $A_{e,b} = 0.01$; $l = 230$ ft; $W = 450\,000$ lb.

The figure indicates that airplanes which simulate effective area shapes 2(a), 2(c), and 4(c) would indeed be expected to produce a nonasymptotic pressure field at the assumed normal operating altitude of 44 000 feet. In fact, for the assumed conditions, the far-field asymptotic variation of bow-shock pressure-rise parameter for these three shapes would not occur until from 220 000 to several million feet from the body. In contrast, note the bow-shock pressures for the tunnel simulated altitude of 4600 feet which are indicated in figure 6. This altitude is near the maximum level which can be simulated in present facilities with a 2-inch model of a transport configuration.

Experimental Investigation of General Theory

The possible sonic-boom advantages indicated by the general theory results of figure 6 have led to an experimental investigation to check the validity of the theory. Pressure measurements were made at a Mach number of 1.414 in the flow field of bodies of revolution representing the shapes and supersonic transport flight condition indicated in figure 6. The pressure data were obtained at a ratio of radial distance to body length of 20 which corresponds to a simulated altitude of 4600 feet for the assumed airplane length of 230 feet. The measured pressure signatures are compared in figure 7 with those obtained from a rigorous application of the theoretical methods of reference 2. From this figure it can be seen that the general theory provides an extremely good representation of the field pressures for all body shapes considered. Although the asymptotic solution is not applicable for this obvious near-field condition, note that the area under the positive pressure region of the general theory and asymptotic signatures are essentially the same. Since this area is related to the positive impulse which would be produced at an observation point by the pressure wave it is an important property damage consideration. On this basis, the lower bound asymptotic shape (shape 4(a)) would produce the lowest positive impulse for a given operating condition.

Calculated Ground Overpressures From Flight at Normal Operating Altitude

From the comparisons in figure 7, the general theory of reference 2 appears to be valid at the simulated near-field wind-tunnel altitude of 4600 feet. It would be anticipated that the general theory is also applicable for the nonasymptotic conditions indicated in figure 6 at the normal operating altitude of 44 000 feet. Furthermore, the asymptotic solution, which is inapplicable at the simulated tunnel altitude of 4600 feet, would be expected to provide a poor approximation of the sonic-boom ground overpressures for the nonasymptotic situation represented by the assumed flight condition.

The theoretical development of reference 2 is based on a uniform atmosphere. In order to determine the sonic-boom ground overpressures from equations (7), (8), and (13), it is first necessary to define a reference pressure which accounts for the variation of atmospheric pressure and temperature between the airplane and the ground. The reference pressure which is the current basis

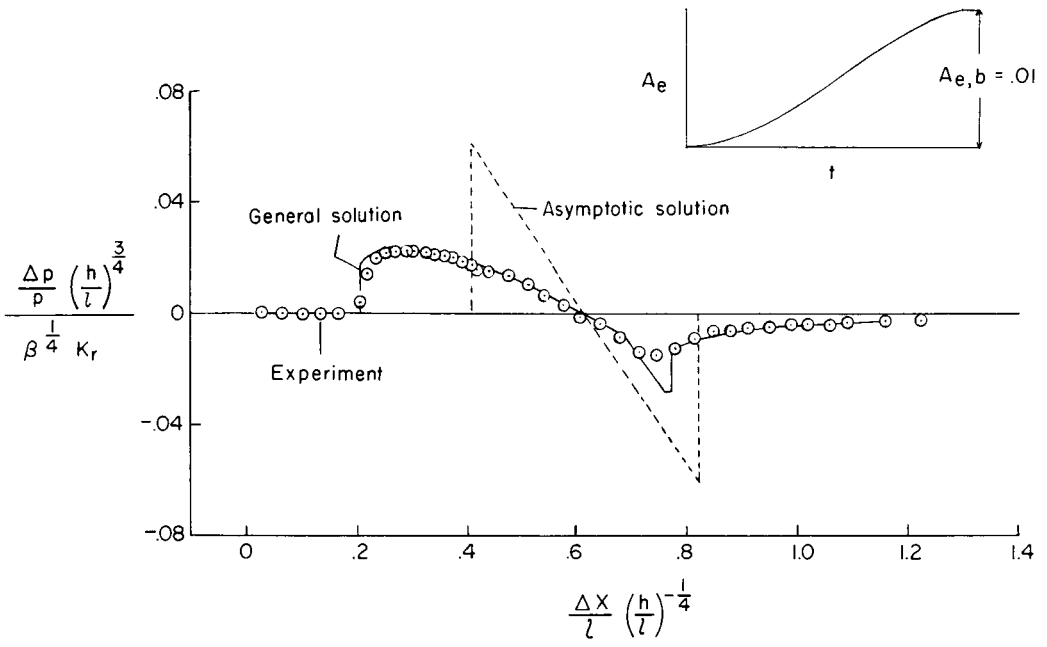

(a) Body shape 2(a).

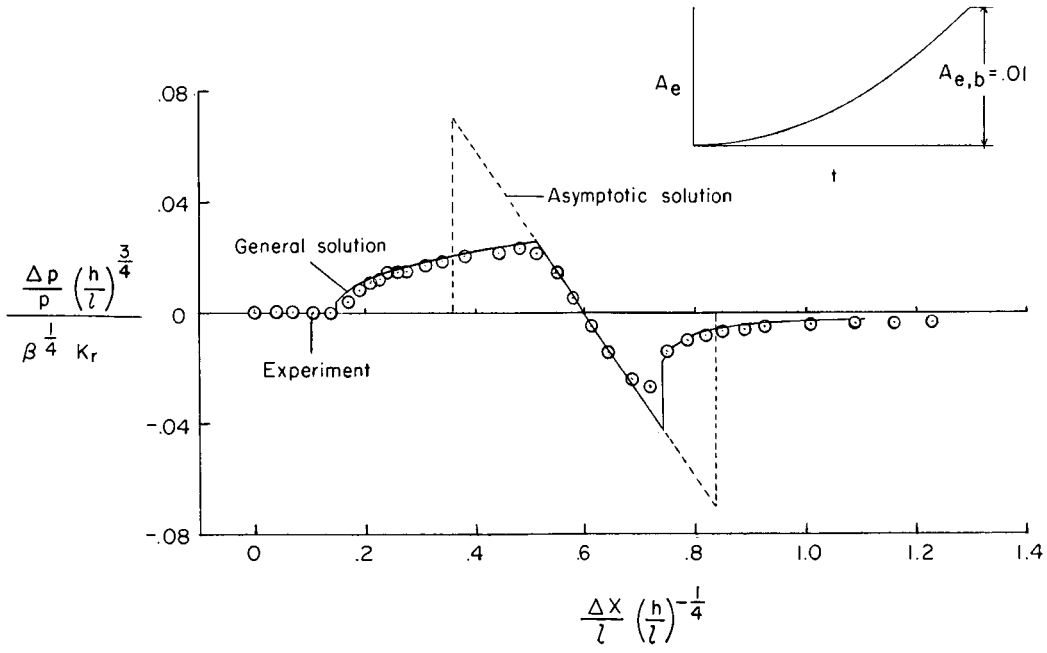

(b) Body shape 2(c).

Figure 7.- Comparison of measured pressure signature with theory for body of revolution scaled to represent typical supersonic transport operating condition. $M = 1.414$; $\frac{h}{l} = 20$.

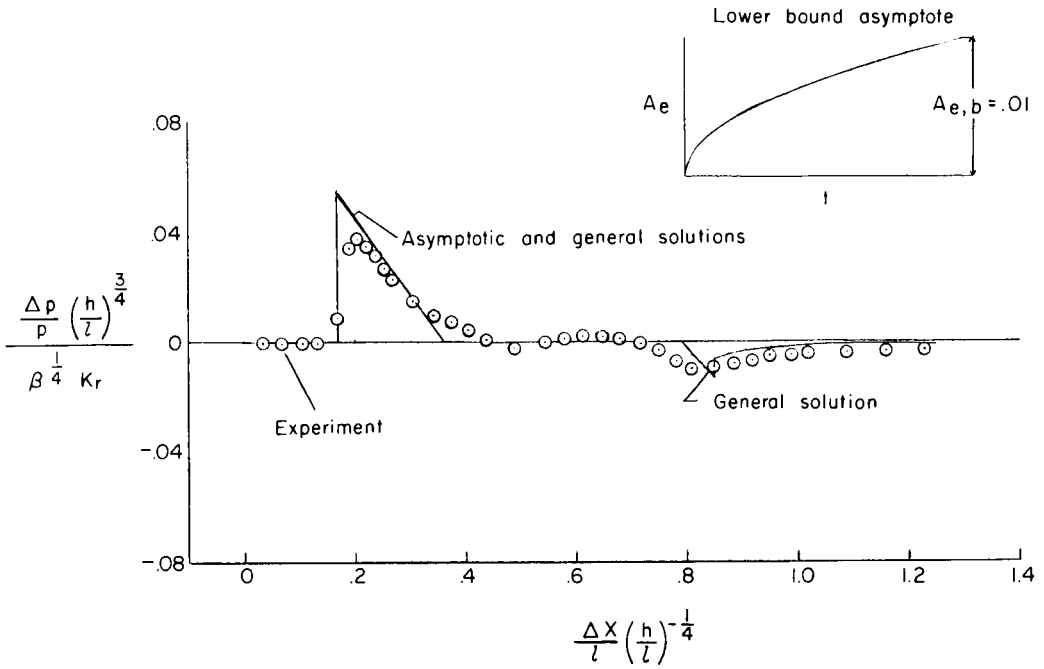

(c) Body shape 4(a).

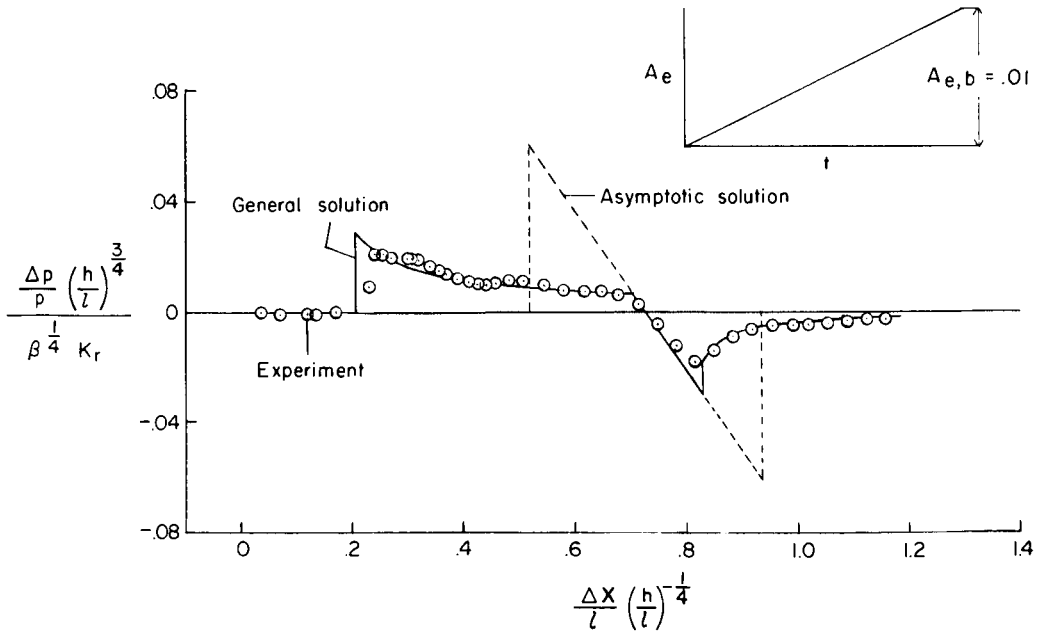

(d) Body shape 4(c).

Figure 7.- Concluded.

for most sonic-boom estimates is $\sqrt{p_a p_g}$, the geometric mean of the pressure at flight altitude and the pressure on the ground. With the use of this geometric mean reference pressure and an established reflection factor, $K_r = 1.9$, the nonasymptotic near-field ground overpressures expected from the body shapes and flight condition of figure 6 may be determined. Representative pressure signatures of this type, for shapes 2(a) and 2(b), are presented in figure 8 and compared with those which would be obtained from asymptotic theory and from the asymptotic lower bound shape (shape 4(a)).

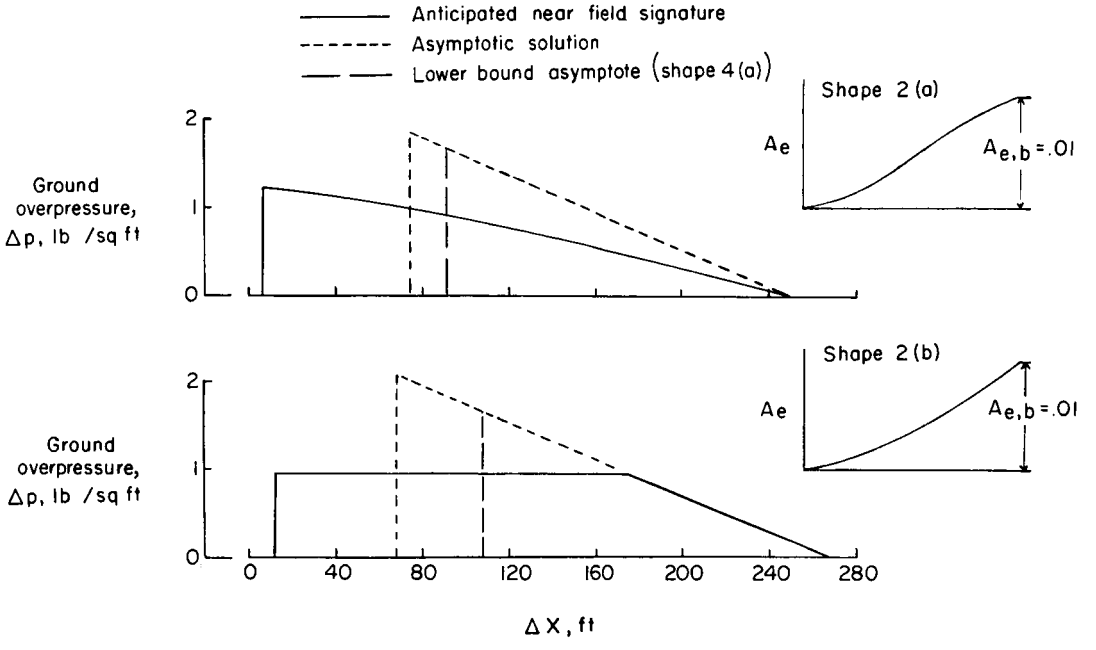

Figure 8.- Comparison of calculated near-field ground overpressures with asymptotic predictions. M = 1.414; h = 44 000 ft; W = 450 000 lb; ℓ = 230 ft.

The calculated results presented in figure 8 indicate distinct alleviation of the sonic boom for effective equivalent body shapes that produce nonasymptotic ground pressure characteristics at normal operating altitudes. The near-field sonic-boom overpressures produced by these shapes are considerably lower than would be expected from asymptotic considerations and indeed are somewhat lower than the lower bound of asymptotic overpressures.

The question as to whether the idealized effective area distributions used herein can be duplicated in a practical airplane configuration can not be answered at this time. However, the present results indicate that, for certain normal operating conditions, a large airplane such as the supersonic transport has the dimensions which tend to place it in a flight region where the currently used asymptotic sonic-boom theory does not apply. The nonasymptotic effects which have been considered suggest that sonic-boom suppression through a design approach to an airplane equivalent body shape which generates near-field pressure characteristics at great distances is a possible solution to the critical sonic-boom problem at transonic acceleration conditions.

CONCLUDING REMARKS

The study of a number of equivalent bodies representing a large airplane at critical transonic flight conditions indicates the possible inapplicability of the asymptotic far-field theory used in current sonic-boom analyses. At these normal operating conditions the pressure field of a large airplane, such as the supersonic transport, tends to exhibit important nonasymptotic near-field effects which must be considered with the use of general theory. Since the shape and magnitude of the near-field pressure signature is dependent on airplane equivalent body shape, sonic-boom suppression through a design approach to a more idealized near-field shape is suggested. The results indicate that if certain effective area distributions can be achieved by real airplanes, sonic-boom overpressures much lower than those predicted by current asymptotic methods would be possible at critical transonic acceleration conditions.

Langley Research Center,
National Aeronautics and Space Administration,
Langley Station, Hampton, Va., May 7, 1965.

REFERENCES

1. Carlson, Harry W.: Correlation of Sonic-Boom Theory With Wind-Tunnel and Flight Measurements. NASA TR R-213, 1964.

2. Whitham, G. B.: The Flow Pattern of a Supersonic Projectile. Commun. Pure Appl. Math., vol. V., no. 3, Aug. 1952, pp. 301-348.

3. Jones, L. B.: Lower Bounds for Sonic Bangs. J. R.A.S. (Tech. Notes), vol. 65, no. 606, June 1961, pp. 433-436.

4. Walkden, F.: The Shock Pattern of a Wing-Body Combination, Far From the Flight Path. Aeron. Quart., vol. IX, pt. 2, May 1958, pp. 164-194.

NASA-Langley, 1965 L-4486